A road map to the detection performance of LFM-PC search radars with CFAR detectors

A road map to the detection performance of LFM-PC search radars with CFAR detectors

Mohamed Samir Abdel Latif Soliman

Chief of EW Department in Military Technical College, Cairo, Egypt.

E-mail. mnna3000@yahoo.com

Abstract. Pulse Compression (PC) radars are used to resolve the problem of designing long range radar systems with excellent range resolution. PC provides radar system with additional processing gain that enhances its detection capability. Among the different types of pulse compression waveforms, Linear Frequency Modulated (LFM) signals are the most tolerant to high Doppler shifts. This is why LFM-PC radars are widely utilized with high speed targets. However, the literature lacks a complete mathematical or simulation model to evaluate the its detection performance. This paper introduces a typical simulation model for search radar that is verified mathematically. The proposed model includes matched filter (MF), moving target detector (MTD), two different constant false alarm rate (CFAR) algorithms and LFM signal sidelobes on radar detection are to be considered. Two simulation models are introduced. Firstly, the Matlab simulation is introduced to verify the mathematical model and the theory. Secondly, the SystemVue simulation is applied to be used in the future work with the hardware in the loop facility.

Keywords. LFM-PC, MF, CFAR, MTD, Matlab, SystemVue Simulation.

1. Introduction

In pulse compression, radar transmits a relatively long pulse that is phase or frequency modulated so that the transmitted bandwidth is larger than an unmodulated pulse with the same duration [1-2]. The pulse duration is chosen to achieve the sufficient transmitted energy required to achieve the desired maximum detection range. In radar receiver, the received pulse is demodulated using a pulse compression filter to yield a narrow pulse with a short duration to achieve the required range resolution. There are various waveforms of pulse compression that a radar designer can choose from according to the radar application requirements. LFM is the best choice for military applications in which detection of high speed fighters is the main concern of radar designers like AN/TPS-59 and AN/FPS-117 [1, 3]. The main disadvantage of LFM waveform is its high range sidelobes compared to other pulse compression waveforms. This can be overcome by applying weighting functions (windows) on the received signal with lower SNR and lower range resolution.

Using LFM within a rectangular pulse compresses the matched filter output by a factor, which is directly proportional to the pulse width and bandwidth. Thus, by using long pulses and wideband LFM modulation, large compression ratios can be achieved. The correlator receiver depends on the fact that the MF is the optimum receiver in presence of noise [4-5]. To reduce the complexity, the MF is implemented in frequency domain. So, the multiplication process is performed instead of the convolution process [6].

In this paper a typical mathematical and simulation model for LFM-PC search radar is introduced. This model can be used as a standard model to evaluate a typical LFM-PC search radar detection performance under different conditions of operations such as different clutter models, different target models, or under effect of different interference or jamming waveforms.

This introduction is the first section of the paper. In the second section, the radar model parameters election is introduced. Third section introduces the Matlab simulation model of the LFM-PC search radar with the corresponding mathematical model. Also, different types of detectors (fixed threshold, CA-CFAR, and GO-CFAR) are applied. Regarding the verification of different detectors, the probability of detection of each detector is compared to the theoretical probability of detection for fixed threshold. Moreover, the effect of four different weighting windows is investigated. The paper presents complete and realistic SystemVue LFM simulation in the fourth section.

2. Radar and target parameters

To choose realistic radar parameters, typical operating radars have been reviewed. Table I summarizes the parameters of most famous and recent operating LFM pulse compression radars [3]. As shown in Table I, the maximum used bandwidth in these radars is 14 MHz. The supposed bandwidth of the proposed radar model is 15 MHz. Moreover; this model has a compression gain of 1500, with 100 μs pulse width, which is much higher than the highest compression gain shown in Table I.

Table I Parameters of operating LFM-PC radars [3]**.**

Radar Model	PRF[Hz]	PW[μ]	BW [MHz]	Date
APS-143C	200, 1500, 88, 400	17	14	2007
STIR	1800, 3600	16	2.5	1995
AWS-6	Not Valid	20	2.5	1997
VARIANT	3000 to 9000	10	6	2003
TRS-3033	Fractions of 5300	2.7	3.7	2003
SPY-I	Not Valid	12.7	10	2012
DA-08	500, 1000	34,68	1.7	2013
DA-08	500,1000	35, 69	1.7	2013
JY-9	790	20	1.3	1990

Target parameters have been chosen to achieve realistic performance for a search-radar target. The range of the target is chosen to be 185.763 Km which is a typical target range for a search radar. The maximum unambiguous range for the proposed radar model is 75 Km, hence, the simulated target range will result in an ambiguous range of 35.763 Km. The assumed target velocity is 21 Km/min which matches many air fighters like F-16, F-22 Raptor, and F-15. Due to radar model PRF, target velocity results in an ambiguous Doppler of 1 KHz instead of unambiguous Doppler of 7 KHz. Another factor affecting the choice of the target range and velocity is the avoidance of range and Doppler straddle. Range or Doppler straddle means that the target return is located between two successive range or Doppler cells [7].

3. Radar Model Simulation and Verification using Matlab

After specifying radar model parameters, a Matlab simulation model has been built. The level of false alarm is assumed to be 10-6 which is a typical value for the most radars [8-9].The target radar cross section (RCS) area is Swerling Case I, i.e., its RCS doesn't change during one scan [1]. The simulation model block diagram is shown in Figure 1.

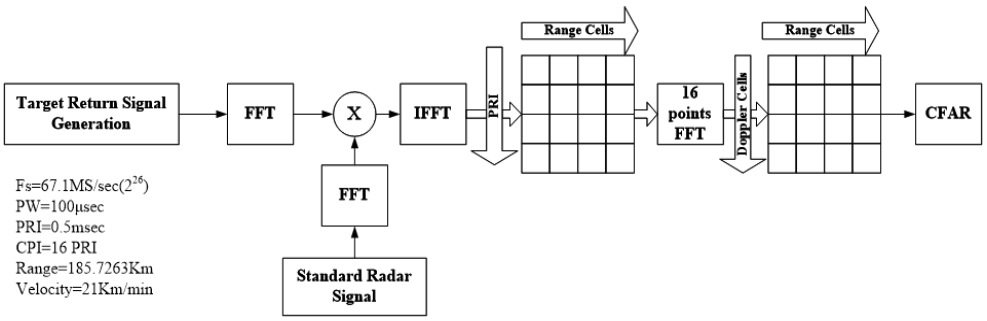

Figure 1 Simulation Block Diagram.

The simulated baseband radar signal is generated for 16 pulse repetition intervals (PRIs) and its Fourier transform is then passed through the MF which is formed in the form of a correlator processor in frequency domain. The output of the MF is then transformed back to the time domain by performing IFFT. In the MTD processor. FFT is performed along the received signal PRIs to generate a matrix with rows are the Doppler cells and with columns are the range cells. The simulated CFAR algorithms are then applied to the resultant matrix for each Doppler cell. To verify the model quantitatively and qualitatively, the signal at the output of each node of the proposed model is simulated and verified with the corresponding mathematical expression.

Radar Signal Verification

Mathematically, the LFM pulse is expressed in time domain as [4]:

$$r(t) = rect\left(\frac{t-T/2}{T}\right) exp(j\pi\mu t^2),\ \mu = \frac{B}{T} \quad (1)$$

where rect( ) is a rectangular function, B is the radar bandwidth and T is the transmitted pulse width. Using Fourier transform, the spectrum of this signal is given by [10]:

$$R(w) = T\sqrt{\frac{1}{BT}}e^{-jw^2/4\pi B}\left\{\frac{[c(x_1)+c(x_2)]+j\,[s(x_1)+s(x_2)]}{\sqrt{2}}\right\} \quad (2)$$

where c(x)and s(x) are the Fresnel integrals.x1 and x2 are defined by:

$$x_1 = \sqrt{\frac{BT}{2}}\left(1+\frac{f}{B/2}\right) and\, x_2 = \sqrt{\frac{BT}{2}}\left(1-\frac{f}{B/2}\right) \quad (3)$$

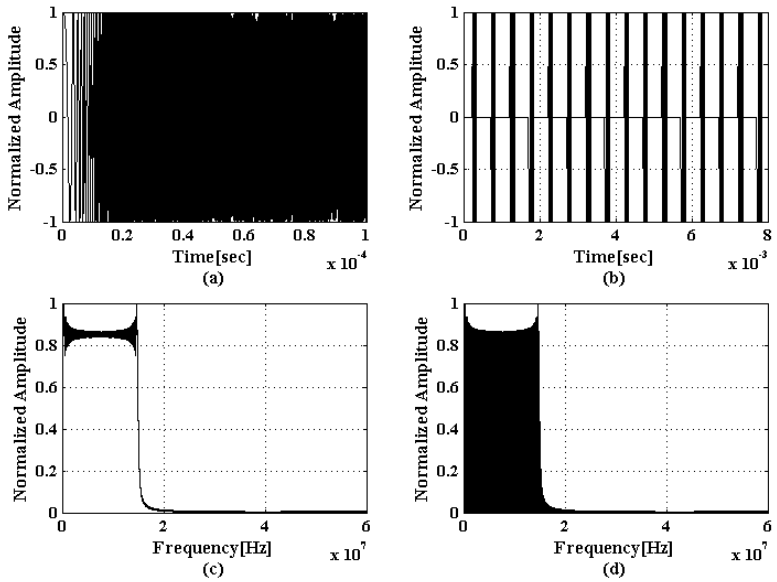

Figure2 Radar signal representation: (a) single pulse in time domain, (b) CPI in time domain, (c) single pulse in frequency domain, (d) train of pulses in frequency domain.

Both time and frequency-domain representations for a single pulse and a pulse train containing 16 pulses are shown in Figure 2.The results shown in Figure 2 (a) and (c) coincide with (b) and (d). The spectrum of radar CPI is similar to that of a single pulse except for the spectral lines appear at multiples of Pulse Repetition Frequency (PRF).

Matched Filter Verification

As stated before, matched filter is formed in the form of a correlator receiver. Matched filter is a linear filter that gives the maximum peak signal power - to - average noise power ratio (SNR) at its output in presence of Gaussian noise for a given waveform [11-12] . The filter impulse response *h(t)* that maximizes signal to noise ratio for the signal r(t) is given by:

$$h(t) = A.r^*(T-t) = A.rect\left(\frac{T/2-t}{T}\right)exp(j\pi\mu(T-t)^2) \quad (4)$$

where (*) denotes the conjugate operator. The value of *A* in (4) depends on the waveform of the signal *r(t)* and it should satisfy the following conditions:

- The peak signal power at the matched filter output to the peak signal power at its input is equal to BT.
- The peak signal power to the average noise power at the output of matched filter is equal to signal energy to the power spectral density of the noise at its output.

The value of *A* that satisfies these conditions is 1.1767.The output SNR of this filter is given by [11]:

$$SNR = \frac{2E}{N_O} \quad (5)$$

where *E* is the input signal energy and $N_O/2$ is the noise power spectral density at the filter input. To verify the improvement factor of the matched filter quantitatively, the peak power of radar signal at the output of the matched filter is calculated and it is compared with peak signal power at the matched filter input with no noise at the input of the matched filter. The improvement factor should be equal to the compression ratio which is supposed to be 31.76 dB in this model. The analysis of continuous time matched filter has been introduced in [10]. The improvement factor achieved in this model is 31.71 dB with a percentage error of 0.1757% from the theoretical improvement factor. The simulation model

proposed in this paper is based on discrete time signals which is explained in [7] where the SNR was deduced to be:

$$SNR = mean\{|s|^2\} \quad (6)$$

where $|s|^2$ is the total signal power and the noise power is assumed to be normalized. The same result can be obtained from Eq.(5). For *N* samples per pulse the sampling frequency is F_s and sampling period is $T_s = 1/F_s$. The average power P_{avg} of the signal of a single pulse is given by [11]:

$$P_{avg} = \frac{1}{N}\sum_{i=1}^{N}|x_i|^2 \quad (7)$$

where x_i is the amplitude of the signal sample *i* of a single pulse. The total energy contained in a single pulse is given by:

$$E_s = T_s \cdot \sum_{i=1}^{N}|x_i|^2 \quad (8)$$

Substituting (8) in (4) :

$$SNR = \frac{T_s.\sum_{i=1}^{N}|x_i|^2}{N_o/2} = \frac{\sum_{i=1}^{N}|x_i|^2}{F_s.N_o/2} = \frac{\sum_{i=1}^{N}|x_i|^2}{P_N} \quad (9)$$

where P_N is the average input noise power which is one in case of normalized AWGN. Eq. (9) states that the SNR at the output of matched filter is given by the total power of the input signal with normalized noise power, in consistency with Eq. (5).To verify the output SNR of the matched filter quantitatively, the SNR at the output of the matched filter is calculated and it is compared with the calculated total input signal power as stated in Eq. (9). Table II provides different calculations at different input signal levels showing the consistency of calculated SNR with the theoretical values.

According to Table II, the total gain introduced to the SNR at the output of the matched filter is 38.7 dB. This value is the sum of the improvement factor introduced for the signal peak power that is 31.7dB and the loss introduced to the input noise average power which is equal to 7dB. The loss of noise power is due to the limitation of its bandwidth from the total sampling rate at the input of the matched filter to the radar bandwidth at the output of the matched filter. To complete the analysis of the matched filter output, the 3-dB width of the output is measured and it is found to be 59.60 ns compared to theoretical 66.67 ns compressed pulse width with a percentage error of 10.59%. This difference is due to sampling accuracy. This error is less than a single sampling period that is 14.9 ns. The normalized output of the matched filter after IFFT block for each PRI is shown in Figure 3. It should be noted that the target appears with one pulse width additional delay according to Eq. (5). Target ambiguous range is 35.7263 km resulting in a time delay of 238.4 μs. As shown in Figure 3, the target has a delay of 338.4 μs (corresponds to range of 50.076 Km ambiguous range) which is equal to the target ambiguous range plus 100 μs corresponds to the matched filter delay.

Table II Comparison between signal energy and SNR at the output of matched filter.

Total signal power[dB]	SNR at output ofMF[dB]	Error percentage[%]
11.9996	11.9880	0.0969
16.9996	16.9857	0.0814
19.9996	19.9900	0.0480
23.9996	23.9898	0.0406
31.9996	31.9636	0.1124

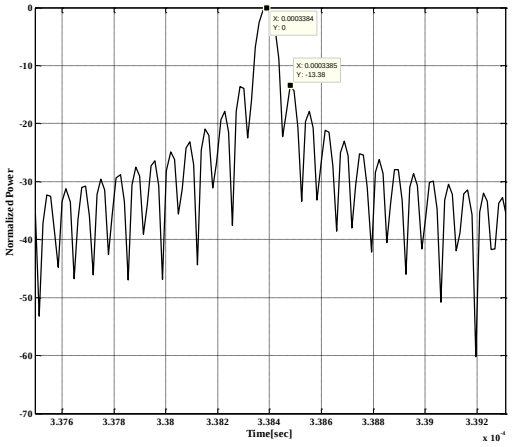

Figure 3 The output of the matched filter output for the LFM signal showing the first sidelobe level.

Radar MTD Verification

After passing through IFFT block, the output of matched filter is passed through MTD processor. The output signal level is increased by the coherent integration gain, which is theoretically 16 or 12.0412 dB in this model. The calculated value for MTD gain in the simulation model is 12.0334 dB with a percentage error less than 0.065%. The output of the MTD block is a 2-D array with rows corresponds to the Doppler cells and columns corresponds to range cells as shown in Figure 4. The target appears at the 9th Doppler cell which means a Doppler frequency between 1000Hz and 1125Hz according to the model Doppler resolution and at range of 50.076 Km. These values is consistent with the ambiguous target Doppler.

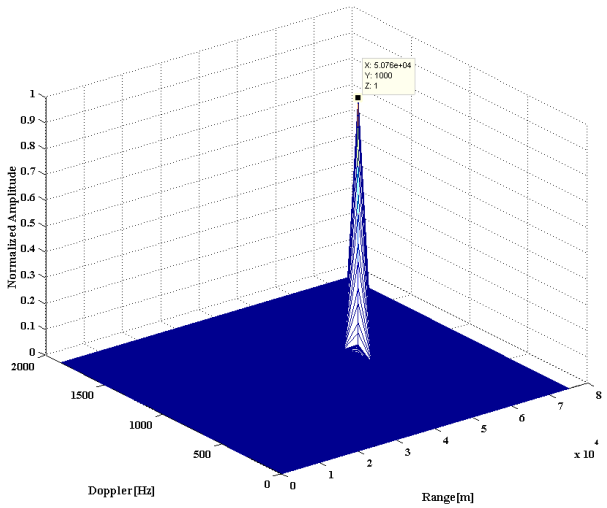

Figure 4 Normalized MTD output**.**

Radar Detection Verification

The output of the MTD block is passed to the CFAR processor. Each Doppler cell is processed by the CFAR block. Each sample of the Doppler cell is compared to its corresponding threshold. The threshold has been set to give a false alarm rate of10-6. This has been done by injecting noise only to the input of the simulated radar system for three types of detectors: fixed threshold, cell average-CFAR (CA-CFAR), and greatest off (GO-CFAR). The window size of both CFAR detectors is 8 range cells. It should be noted that CFAR processor introduces additional delay corresponding to the window cells that precede the target and the preceding guard cell which is equivalent to 0.53644 μs or 80.4663 m range. Taking

into account the delay due to matched filter, the total delay is 100.53644 μs or 15.08 Km. This delay can be compensated in the radar display. Based on Neyman-Pearson criterion, radar probability of detection PD is given by [13]:

$$P_D = 0.5 \times erfc\left(\sqrt{-ln(P_{fa})} - \sqrt{SNR + 0.5}\right) \quad (10)$$

where P_{fa} is the probability of false alarm, and erfc( )is the complementary error function and it is given by [10]:

$$erfc(x) = 1 - \frac{2}{\sqrt{\pi}}\int_0^x e^{-z^2}\,dz \quad (11)$$

Recalling the gain of each processing stage in the radar model, the detection advantage of the MF over the theoretical envelope detector with 38.7 dB can be expected and an advantage of 12 dB for the MTD over the matched filter. The overall processing gain is expected to be 50.7 dB. This means that the prospective detection performance of the radar model should be enhanced with the overall model processing gain. To investigate the enhancement of the model detection performance, the detection probability has been calculated at the output matched filter and MTD of the radar simulation model at different SNR values. To be consistent with theoretical values, the simulation has been done with the fixed threshold detector taking into account the processing gain of each stage. The results are depicted in Figure 5. It shows how the simulation results coincide with the theoretical values calculated for the improvement in the SNR in the matched filter and MTD.

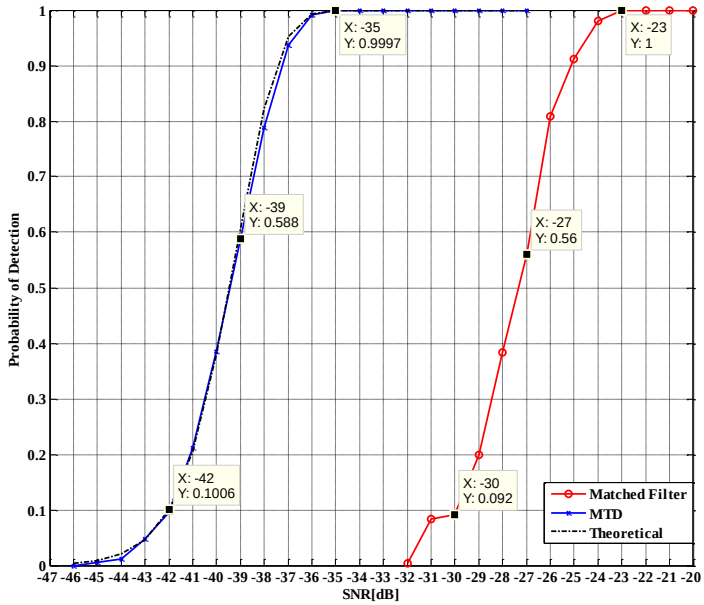

Figure 5 Radar detection at different stages compared with theoretical detection**.**

After verifying the simulation model detection with the fixed threshold detector, both CFAR detectors are investigated in Figure 6. It reveals that both the CFAR detectors have lower detection than the fixed threshold detector. It is manifest that the difference between the two types of detectors (fixed and CFAR) is the method of forming the threshold. The fixed threshold detector sets the value of the threshold at a constant value that gives certain false alarm rate. This value is calculated depending on the noise only and does not change with the change in the received signal. On the contrary, the threshold in CFAR detectors is adapted according to the received signal, which contains sidelobes, to maintain constant false alarm rate. So, the sidelobes affect the detection of CFAR detectors.

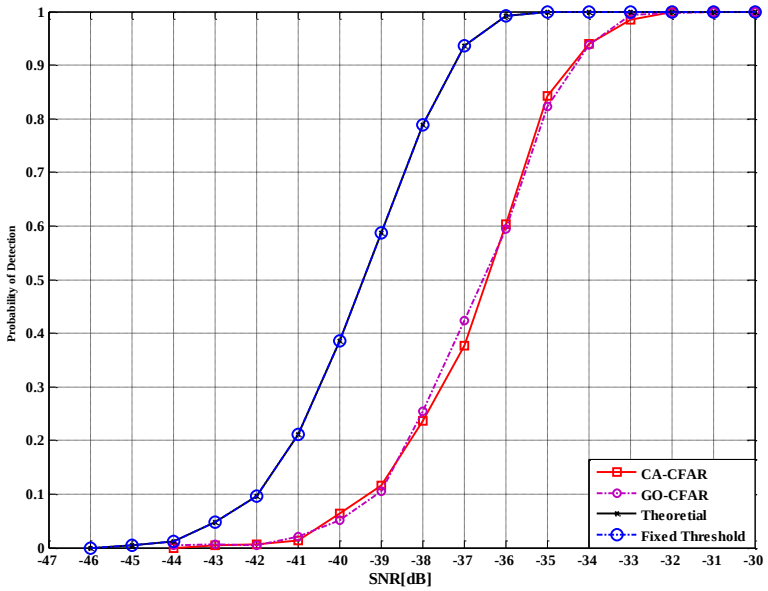

Figure 6 Detection of fixed threshold and CFAR detectors compared to theoretical detection**.**

To investigate the effect of sidelobes on the fixed threshold detector, the fixed threshold is recalculated with the presence of sidelobes plus noise. This is done by calculating the fixed threshold value after considering the sidelobes outside the locations of the guard cells of CFAR detectors. In this way, the calculation basis for CFAR detectors and fixed threshold detector is the same. The injected sidelobes were chosen at SNR=-32 dB which is the maximum SNR value in the detection curve. By choosing this value, a false alarm rate of 10^{-6} is guaranteed on the whole range of the SNR values of the simulation. To this extent, the only difference between the two types of the discussed detectors is the adaptability feature in CFAR detectors. The detection performance of the fixed threshold detector with and without sidelobes is shown in Figure 7. It shows how the detection calculated with the first threshold (calculated without sidelobes) matches the theoretical results. However, the false alarm rate is increased due to sidelobes to 10^{-5} instead of 10^{-6}. The detection calculated with the second threshold (calculated with sidelobes), based on the presence of the sidelobes, reveals how sidelobes of LFM signal affects radar detection. To maintain a false alarm rate of 10^{-6} at this level of sidelobes, threshold is raised and, consequently; detection is lowered.

The target return output is then multiplied by a rectangular window that passes the main lobe of the target return and nulls all the surrounding sidelobes. The output of the matched filter can be expressed as:

$$y[n] = (x_t[n] * h[n]).w[n] + (x_{noise}[n] * h[n]), w[n] = rect\left(\frac{n-M}{L}\right) \quad (12)$$

where y[n]is the matched filter output, xt[n] is the target return signal, (*) is a convolution, h[n] is the impulse response of the matched filter, w[n] is the rectangular window, $x_{noise}[n]$is the noise signal, M is the target delay at the matched filter output, L is the total number of samples of the filter output.

The detection of both CFAR detectors (CA-CFAR and GO-CFAR) with and without sidelobes compared to the fixed threshold detector is shown in Figure 8. It is clear that the CFAR detection introduces loss to the target sensitivity compared to the fixed threshold detector. The loss is within the theoretical value for the simulated parameters of CFAR detectors [1]. It is also obvious that the loss due to sidelobes is apparent at higher SNR values where sidelobe level is higher than the noise floor.

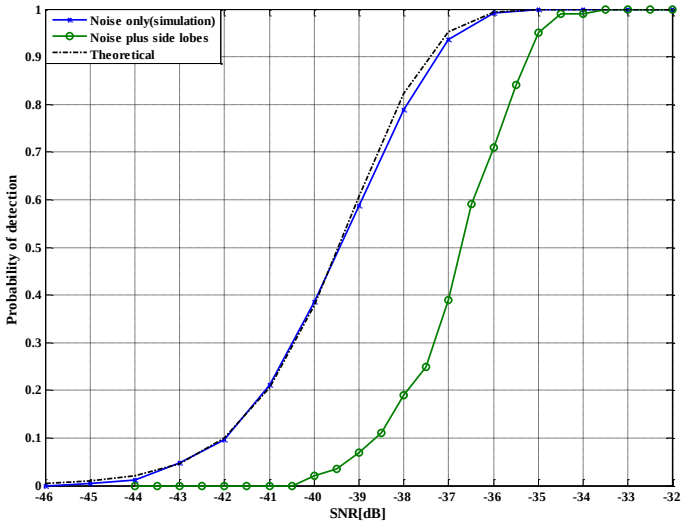

Figure 7 Radar detection with two different fixed thresholds.

Figure 8 shows that both CA-CFAR and GO-CFAR curves are shifted from the fixed threshold curve. It can be seen that the detection of both CFAR techniques is higher than that of the theoretical and fixed threshold curves before the value of SNR=-37 dB. Beyond this point, the detection of both CFAR processors is lower than that of theoretical detection. The side lobes of the target return that appear in the CFAR processor window affect the CFAR threshold. When the level of these side lobes is below certain level, the CFAR threshold is lower than the fixed threshold. This is why the detection of CFAR processors is better than the fixed threshold. This is discussed in full detail in [13].

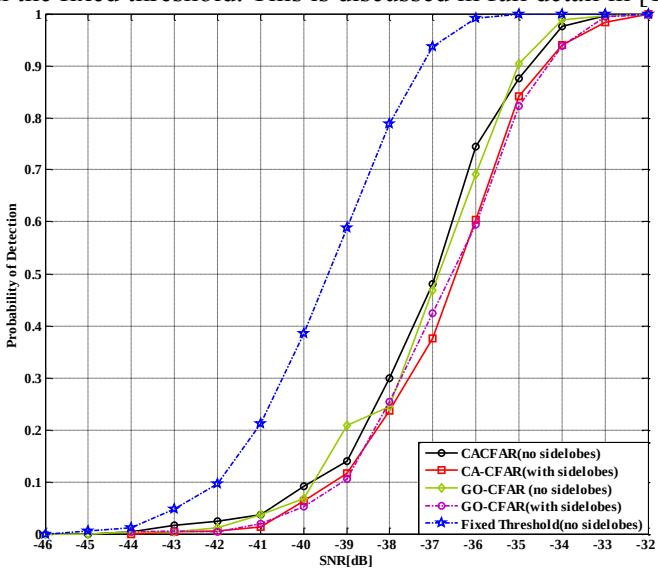

Figure 8 Detection curves of CFAR detectors with and without sidelobes effect**.**

Figure 9 illustrates the effect of side lobes on CFAR and fixed threshold detectors. To investigate this effect, the target return is injected at the radar input without noise. Figure 9 (a) shows the fixed threshold, CA-CFAR, and GO-CFAR thresholds at signal power of -38dB (just before SNR=-37dB). It is obvious that fixed threshold has a higher value than the value of both CFAR thresholds at the target cell. On the other hand, at signal level of -28dB, Figure 9 (b) shows how the fixed threshold has a lower value than that of the two CFAR detectors at the target cell. This gives a reason for the detection performance shown in Figure 8.

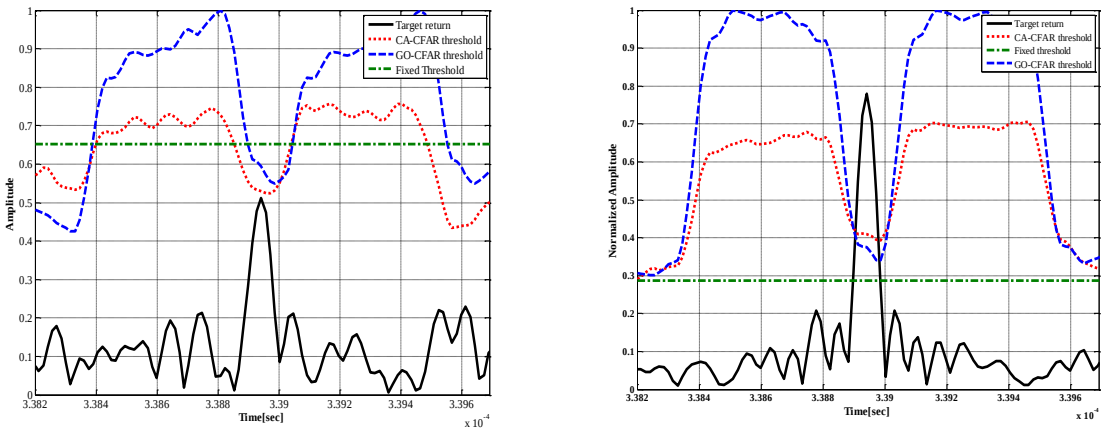

(a) signal power=-38dBm (b) signal power=-28 dBm

Figure 9 Threshold of different detectors with sidelobes only**.**

Effect of Weighting Windows on Radar Detection

Weighting windows are used with LFM signals to reduce range sidelobes level at the expense of SNR [12]. The use of weighting windows, in turn, affects radar probability of detection. To evaluate the effect of weighting windows on radar detection, different window types have been simulated and radar probability of detection has been calculated for each window at different SNR values. The simulated windows are Hanning, Hamming, Kaiser, and Chebyshev windows. Radar detection with Hamming, Hanning, Kaiser, and Chebyshev windows is shown in Figure 10.Hamming and Hanning windows introduce moderate sidelobe attenuation with moderate mainlobe level reduction and width widening [10]. On the other hand; Kaiser and Chebychev windows introduce high sidelobe attenuation with the cost of high level reduction and width increase of mainlobe. By the choice of these windows maximum and minimum weighting effects are considered. One can conclude that the higher the sidelobe attenuation, the lower the radar detection. This is because the attenuation of sidelobe level is accompanied with mainlobe-level reduction as well.

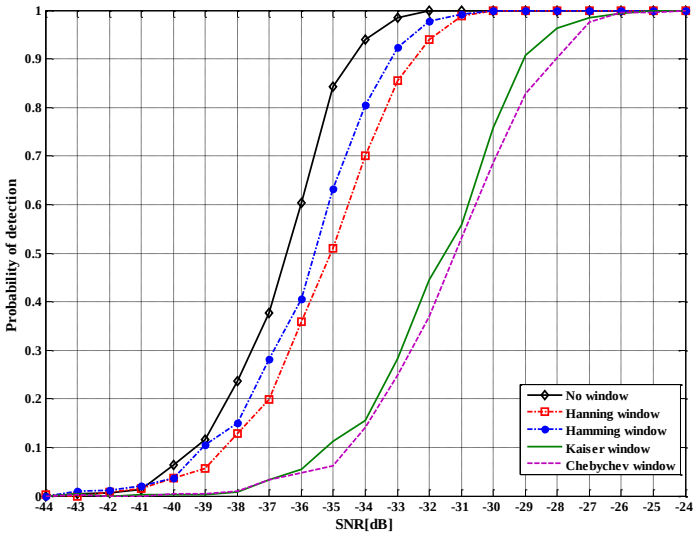

Figure 10 Radar detection with different window types using CA-CFAR.

4. Radar Model Simulation and Verification using Matlab

To be more convinced a Complete LFM pulse compression search radar model is built in this paper using SystemVue. The entire mentioned signal processing techniques is used to simulate LFM-PC radar similar to the working LFM-PC radars. This model helps to create realistic scenario of search radar environment and to have a platform for general hardware in the loop testing and evaluating any jamming

techniques performance. After ensuring the functionality of the model the SystemVue LFM-PC model can be replaced by another designed LFM-PC model using FPGA.

LFM-PC Model Parameters

Realistic parameters for the modern LFM-PC are chosen. Therefore, the model has a high range resolution and also high immunity against jamming signal. Pulse Repetition Interval (PRI) is chosen to be five times the PW (PRI set to be 500 ms) which is considered reasonable value for a search radar. The LFM-PC model set to use LPRF to give the model the ability to work with high compression ratio, which is the paper main concern [14]. Since the bandwidth of the LFM-PC is set to be 15MHz, the Sampling frequency is set to 67MHz to be more than twice the bandwidth according to Nyquist theorem. The carrier frequency of the model is very essential to calculate the Doppler shift for the simulated target [10], carrier frequency is set to be 3GHz to be similar to most of ground radars working in S band. The CFAR in the model is using two common algorithms as stated before.

SystemVue Radar Modeling

The SystemVue 2015.1 software developed by Keysight with the radar library saves development time and verification expense in research and development for complex radar system algorithm developers, architects, and system verifiers. It can be used for modelling different types of complex radar systems for creating realistic working radar scenarios, including the transmitter blocks, processing blocks, receiver blocks and environmental effect items. Environmental effect items include targets and radar cross section (RCS) different algorithm, intentional and non- intentional interference, and the effect of various signal processing algorithms. The block diagram of the Radar Model is built on SystemVue Ver. 2015.1 as shown in Figure 11. The LFM-PC radar model block diagram is discussed in details as follows. The output signal from LFM-PC generator in the time domain and frequency domain is shown in Figure 12. This LFM signal is a complex signal has both In-phase (I) component and Quadrature (Q) component. The LFM-PC baseband generated signal is up converted with 3 GHz carrier frequency. The Simulation results for LFM-PC agree with theoretical results [15]. All the radar parameters is selected to verify the Matlab simulation.

Secondly, set sample rate module as shown in Figure 11 (a). It is only responsible for ensuring that the sampling frequency is equal to the sampling frequency of the successor stage. The third module is complex to envelop converter. It converts the input complex signal (Cx) to complex envelop (ENV) at the output. The carrier frequency is represented by Fc = 3GHz. Finally, the amplifier is used to normalize the output power. Figure 11(b) shows the target and noise models. The target model is used to simulate the target radar cross section, target speed and target distance. The target model in this system is acting as a virtual antenna which reflects radar transmitted signal back to radar receiver. The target sub network simulates the target model for radar system with RCS, transmission delay, transmission loss and Doppler shift. Five Swerling models are supported for target RCS fluctuation [10]. Swerling Case I is selected as the Matlab simulation. The propagation effect is put into consideration. The Doppler shift is then added. Finally, transmission delay caused by target distance is added. Noise Density module, gives the radar model realistic environment condition. The effect of the noise is added to the transmitted signal to simulate the noise in the channel. This model is controlling the noise level comparing to signal. The noise power in the channel is varied according to the required. The noise power is constant over signal bandwidth. Figure 11(c) shows the radar receiver model. Demodulator module, acts as coherent demodulator that is used to perform amplitude, phase, frequency, or I/Q demodulation. Rec. To CX module changes the signal from real and imaginary form to complex form. Radar Pulse Compression Filter module is responsible for compressing the received pulse and hence increase the range resolution. Figure 11(d) shows the PC filter is actually a matched filter follows by filter to reduce the LFM sidelobes level [16].

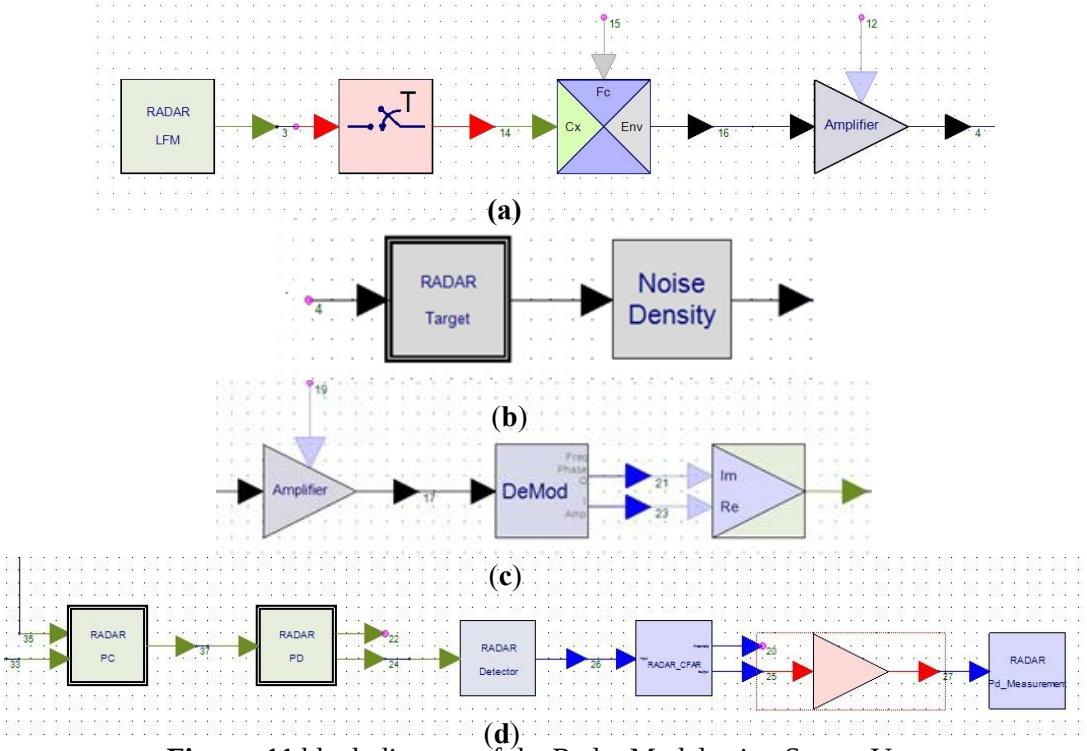

Figure 11 block diagram of the Radar Model using SystemVue**.**

The reflected signal from the target enters the PC-filter from port SigIn and the reference signal in frequency domain is entered to the filter from RfIn port. Matched filter is considered as a linear process performing auto correlation between the received signal and the reference signal. The matched filter converts the signal from time domain to frequency domain using FFT model to perform multiplicative process instead of convolution process which is more complicated. After performing the multiplicative process with the reversed complex conjugate of reference signal the output is converted back to time domain using FFT model working in the inverse mode (IFFT). The first side lobe level of matched filter output of the simulated LFM signal is -13.426dB as shown in Figure 13. It is concurrent with the Matlab simulation results shown in Figure 3.

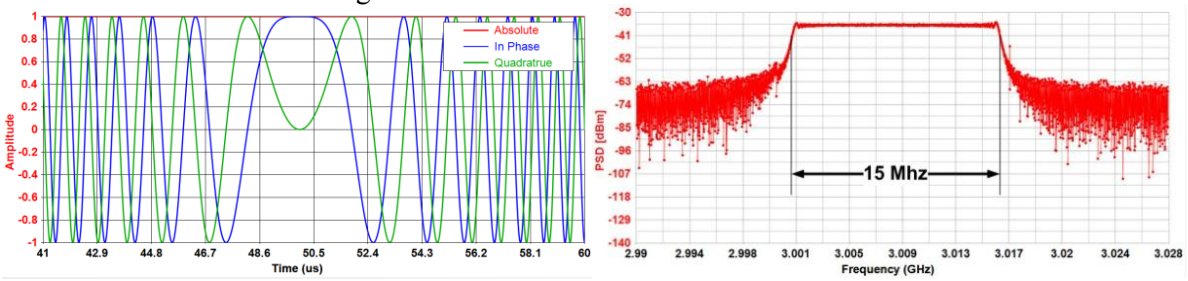

Figure 12 LFM-PC radar output in time domain and Frequency domain.

The implementation of MTD is based on FFT over same range gate data of different PRI. The coherent integration of CPI increases the signal output level theoretically by 12.04 dB. In this model it is measured and it is equal to 12.03. The MTD output is shown in Figure 14. The target appears at the 9th Doppler cell which means a Doppler frequency between 1000Hz and 1125Hz. This value is consistent with the ambiguous target Doppler.

Radar Detector module is used for video signal detection. The detector type is set to the default setting (square detector) which gives the best radar performance. The CFAR processor which is responsible for adapting the false alarm as a constant while the noise and the clutter varies. CFAR model

processes every Doppler cell. The samples out of the CFAR are compared to the pre-setting threshold. From Figure 15, it obvious that the CFAR utilizes adaptive threshold according to the used algorithm.

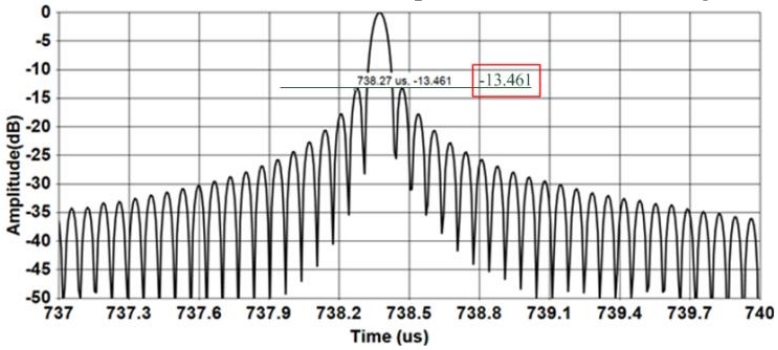

Figure 13 LFM First Sidelobe Level at -13.461 dB.

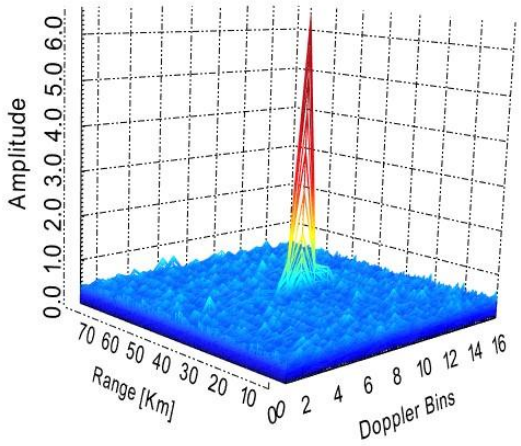

Figure 14 MTD output.

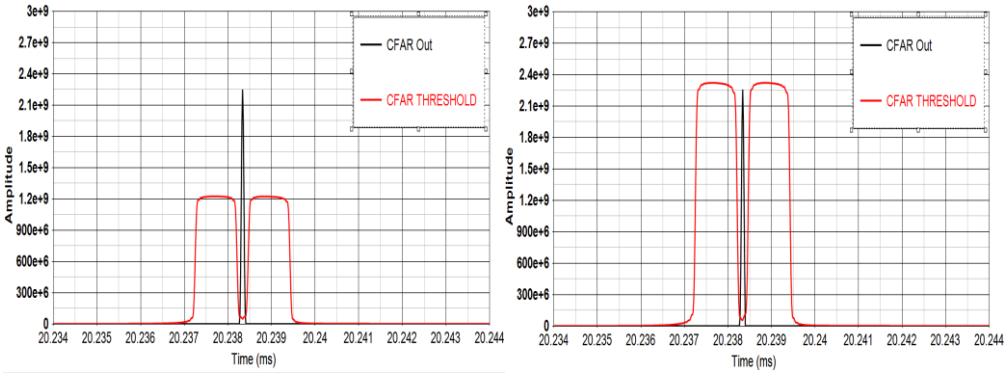

(a)CA-CFAR-Output-Signal (b) LFM Pulse in frequency domain

Figure 15 LFM radar signal.

3D representation of the CA-CFAR processor is shown in Figure 16. It's clear that the CFAR successfully eliminate the background noise. Radar probability of detection (PD) module is responsible for estimating the radar model PD based on radar video signal. The total simulation samples length is given by:

$$Simnum = PRI - Num \times FFT - Size \times DetectionNum \quad (13)$$

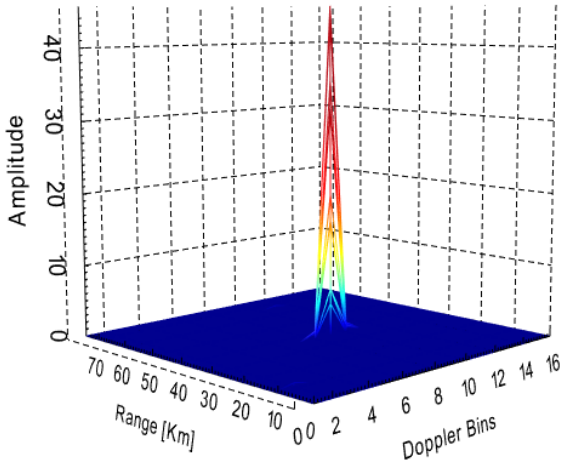

Figure 16 CA-CFAR 3D Output.

So the simulation samples is = 160,800,000 samples. The probability of detection is estimated based on Mont Carlo estimation algorithm as:

$$P_D = \frac{1}{Simnum}\sum_{S=1}^{Simnum} D(S) \quad (14)$$

where *D(S)* refers to the detection event based on binary hypothecs:

$$D(t) = \begin{cases} 1 & Right\ detection \quad H_1 \\ 0 & Missdetection \quad H_0 \end{cases} \quad (15)$$

where, $H_1$and H_0 represent radar target is detected with an actual target presented (right decision) and no target detected while actual target at the input (miss detection) respectively.

Weighting Windows Effect on Radar Model Detection

The weighting windows Kaiser, Bartlett, Hanning, Hamming, Blackman and Step Blackman are used. The weighting windows equation and analysis are discussed in details in [17]. The time-domain representation of these windows is shown in Figure 17.

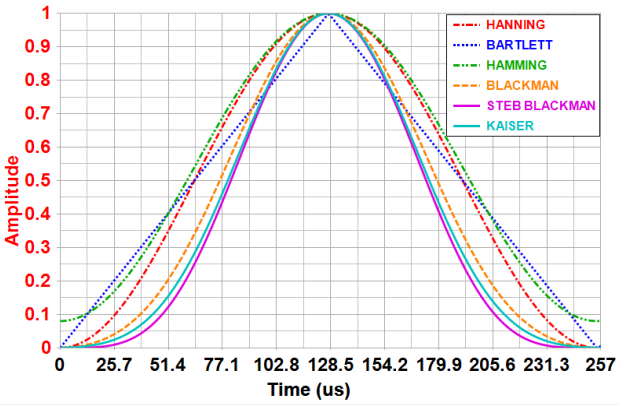

Figure 17 Weighting Windows Time-Domain

Figure 18 shows the Effect of different window on radar detection using CFAR. From Figure 18 and Figure 18 it's noticed the higher sidelobe attenuation given by the applied window, the lower the radar detection. The explanation of this notice is attenuation of sidelobes has direct impact on main lobe reduction as well. No window and Kaiser Window Hamming introduce low side lobe attenuation with

low mainlobe level reduction. These results are the same as the Matlab simulation shown in Fig 10. Thus, the SystemVue model is succeeded to verify a realistic LFM radar model.

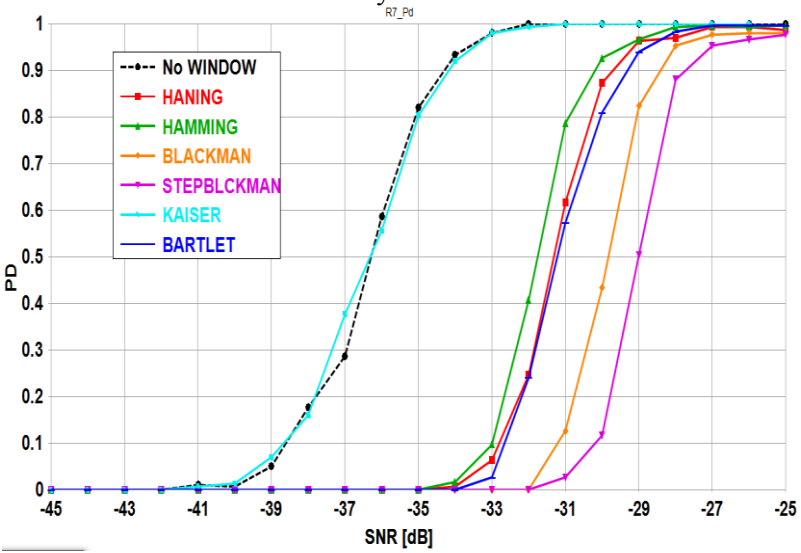

Figure 18 Effect of Different Window on Radar Detection using CFAR

5. Conclusion

In this paper, a simulation model for an LFM-PC radar is introduced and verified by Matlab and SystemVue. The parameters of the proposed radar model have been chosen to match that of the operating LFM-PC radars. The proposed radar model has the highest compression gain compared to the similar radar systems.

The verification process of the proposed model has compared the output of each stage with the corresponding mathematical output. The matched filter output has been verified from different points of view. The first is the gain provided for the input peak signal power. The second point of view is the SNR at the output of the matched filter. The theoretical value of SNR for discrete time signals has been proved with two different approaches. The two approaches led to the same result that is consistent with simulation results. The width of the output pulse of the matched filter has been compared to the theoretical one and it is found to be approximately the same. The simulated MTD processor introduces additional 12dB gain just as the supposed theoretical gain value.

It has been found that the sidelobes of LFM signal has two effects on radar detection. The first is lowering radar detection as a result of the increase in threshold to maintain 10^{-6} false alarm rate. This is true for fixed threshold, CA-CFAR, and GO-CFAR. The second effect is on CFAR detection performance. It has been shown that both CFAR techniques introduce gain to radar detection before a certain value of SNR. This value is -37dB. At higher values of SNR, both CFAR techniques introduce loss to radar detection. This loss is less than 1dB. It has been also found that the use of weighting windows lowers radar detection with a loss that depends on the sidelobe.

6. References

[1] M. Skolnik, Radar Handbook, Third Edition: McGraw-Hill Education, 2008.
[2] L. Kocjancic, et al., "Multibeam radar based on linear frequency modulated waveform diversity," IET Radar, Sonar & Navigation, vol. 12, pp. 1320-1329, 2018.
[3] N. Friedman, "the naval institute guide to world naval weapons systems," naval instiute press, 2006.
[4] N. Levanon and E. Mozeson, Radar Signals: Wiley, 2004.
[5] M. A. B. Othman, et al., "Performance Analysis of Matched Filter Bank for Detection of Linear Frequency Modulated Chirp Signals," IEEE Transactions on Aerospace and Electronic Systems, vol. 53, pp. 41-54, 2017.

[6] A. S. T. P. a. K.Tanuja, "Design of matched filter for radar applications," electrical and electronics engineering: An International Journal (ELELIJ), vol. 3, p. 10, November 2014.
[7] G. Galati and E. Institution of Electrical, Advanced Radar Techniques and Systems: Peter Peregrinus, 1993.
[8] M. Kolawole, "Peak Detection and Tracking," in Radar Systems, ed: Newnes, 2002.
[9] J. s. j. s. a. W. H. M. A. Richards, Principles of Modern Radar: SciTech Publishing, Incorporated, 2010.
[10] B.R.Mahafza, Radar Systems, analysis and design using Matlab: CHAPMAN & Hall, 2000.
[11] B.C.Levy, Principles of Signal Detection and Parameter Estimation: Springer, 2008.
[12] C.Kumar, "Development of efficient Radar Pulse Compression Technique," Master, National Institute of Technology Rourkela, 2014.
[13] I. B. Antipov, John, "Estimation of a Constant False Alarm Rate Processing Loss for a High-Resolution Maritime Radar System," DEFENCE SCIENCE AND TECHNOLOGY ORGANISATION, EDINBURGH, AUSTRALIA,2008.
[14] H.Meikle, Modern Radar Systems: Artech House, 2008.
[15] D. Adamy, EW 101: A first course in electronic warfare vol. 101: Artech House, 2001.
[16] A. D. Martino, Introduction to modern EW systems: Artech house, 2012.
[17] M. B. S. R. N. Lothes, and R. G. Wiley, Radar vulnerability to jamming. Norwood, MA: Artech House, 1990.